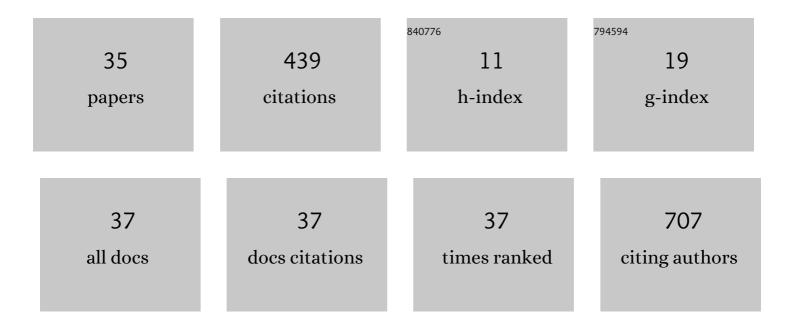
## **Tobias Wech**

List of Publications by Year in descending order

Source: https://exaly.com/author-pdf/3742782/publications.pdf Version: 2024-02-01



TOBIAS WECH

#	Article	IF	CITATIONS
1	A dataâ€driven semantic segmentation model for direct cardiac functional analysis based on undersampled radial MR cine series. Magnetic Resonance in Medicine, 2022, 87, 972-983.	3.0	2
2	Evaluation of combined late gadoliniumâ€enhancement and functional cardiac magnetic resonance imaging using spiral realâ€ŧime acquisition. NMR in Biomedicine, 2022, 35, e4732.	2.8	2
3	Realâ€time cardiac <scp>MRI</scp> using an undersampled spiral kâ€space trajectory and a reconstruction based on a variational network. Magnetic Resonance in Medicine, 2022, 88, 2167-2178.	3.0	5
4	Accelerated aortic 4D flow MRI with wave AIPI. Magnetic Resonance in Medicine, 2021, 85, 2595-2607.	3.0	4
5	Cardiac realâ€ŧime MRI using a preâ€emphasized spiral acquisition based on the gradient system transfer function. Magnetic Resonance in Medicine, 2021, 85, 2747-2760.	3.0	11
6	Deep learning-based segmentation of the lung in MR-images acquired by a stack-of-spirals trajectory at ultra-short echo-times. BMC Medical Imaging, 2021, 21, 79.	2.7	7
7	Deep learningâ€based cardiac cine segmentation: Transfer learning application to 7T ultrahighâ€field MRI. Magnetic Resonance in Medicine, 2021, 86, 2179-2191.	3.0	14
8	Non-contrast pulmonary perfusion MRI in patients with cystic fibrosis. European Journal of Radiology, 2021, 139, 109653.	2.6	6
9	Self-configuring nnU-net pipeline enables fully automatic infarct segmentation in late enhancement MRI after myocardial infarction. European Journal of Radiology, 2021, 141, 109817.	2.6	10
10	The temperature dependence of gradient system response characteristics. Magnetic Resonance in Medicine, 2020, 83, 1519-1527.	3.0	11
11	Freeâ€breathing selfâ€gated 4D lung MRI using waveâ€CAIPI. Magnetic Resonance in Medicine, 2020, 84, 3223-3233.	3.0	12
12	Field camera versus phantom-based measurement of the gradient system transfer function (GSTF) with dwell time compensation. Magnetic Resonance Imaging, 2020, 71, 125-131.	1.8	3
13	A compressed sensing accelerated radial MS-CAIPIRINHA technique for extended anatomical coverage in myocardial perfusion studies on PET/MR systems. Physica Medica, 2019, 64, 157-165.	0.7	4
14	Realâ€ŧime Triggered RAdial Single‣hot Inversion recovery for arrhythmiaâ€insensitive myocardial T1 mapping: motion phantom validation and in vivo comparison. Magnetic Resonance in Medicine, 2019, 81, 1714-1725.	3.0	2
15	Power-Doppler perfusion phenotype in RA patients is dependent on anti-citrullinated peptide antibody status, not on rheumatoid factor. Rheumatology International, 2019, 39, 1019-1025.	3.0	3
16	UTE‧ENCEFUL: first results for 3D highâ€resolution lung ventilation imaging. Magnetic Resonance in Medicine, 2019, 81, 2464-2473.	3.0	37
17	Gradient waveform preâ€emphasis based on the gradient system transfer function. Magnetic Resonance in Medicine, 2018, 80, 1521-1532.	3.0	24
18	Robust motion correction in CEST imaging exploiting lowâ€rank approximation of the zâ€spectrum. Magnetic Resonance in Medicine, 2018, 80, 1979-1988.	3.0	16

TOBIAS WECH

#	Article	IF	CITATIONS
19	Single-shot late Gd enhancement imaging of myocardial infarction with retrospectively adjustable contrast and heart-phase. Magnetic Resonance Imaging, 2018, 47, 48-53.	1.8	4
20	Frequency-modulated bSSFP for phase-sensitive separation of water and fat. Magnetic Resonance Imaging, 2018, 53, 82-88.	1.8	0
21	Multifrequency reconstruction for frequencyâ€modulated b <scp>SSFP</scp> . Magnetic Resonance in Medicine, 2017, 78, 2226-2235.	3.0	6
22	Comparison of Turbo Spin Echo and Echo Planar Imaging for intravoxel incoherent motion and diffusion tensor imaging of the kidney at 3 Tesla. Zeitschrift Fur Medizinische Physik, 2017, 27, 193-201.	1.5	6
23	Anti-CCP status determines the power Doppler oscillation pattern in rheumatoid arthritis: a prospective study. Rheumatology International, 2016, 36, 1671-1675.	3.0	4
24	An intravoxel oriented flow model for diffusionâ€weighted imaging of the kidney. NMR in Biomedicine, 2016, 29, 1403-1413.	2.8	25
25	Development of Real-Time Magnetic Resonance Imaging of Mouse Hearts at 9.4 Tesla— Simulations and First Application. IEEE Transactions on Medical Imaging, 2016, 35, 912-920.	8.9	10
26	Using self-consistency for an iterative trajectory adjustment (SCITA). Magnetic Resonance in Medicine, 2015, 73, 1151-1157.	3.0	15
27	Model-Based Acceleration of Look-Locker T1 Mapping. PLoS ONE, 2015, 10, e0122611.	2.5	24
28	High resolution myocardial first-pass perfusion imaging with extended anatomic coverage. Journal of Magnetic Resonance Imaging, 2014, 39, 1575-1587.	3.4	28
29	Measurement accuracy of different active tracking sequences for interventional MRI. Journal of Magnetic Resonance Imaging, 2014, 40, 490-495.	3.4	6
30	Consideration of slice profiles in inversion recovery Look–Locker relaxation parameter mapping. Magnetic Resonance Imaging, 2014, 32, 1021-1030.	1.8	10
31	Accelerated radial Fourier-velocity encoding using compressed sensing. Zeitschrift Fur Medizinische Physik, 2014, 24, 190-200.	1.5	5
32	Whole-Heart Cine MRI in a Single Breath-Hold – AÂCompressed Sensing Accelerated 3D Acquisition TechniqueÂfor Assessment of Cardiac Function. RoFo Fortschritte Auf Dem Gebiet Der Rontgenstrahlen Und Der Bildgebenden Verfahren, 2013, 186, 37-41.	1.3	18
33	Modelâ€based Acceleration of Parameter mapping (MAP) for saturation prepared radially acquired data. Magnetic Resonance in Medicine, 2013, 70, 1524-1534.	3.0	33
34	Resolution evaluation of MR images reconstructed by iterative thresholding algorithms for compressed sensing. Medical Physics, 2012, 39, 4328-4338.	3.0	20
35	Accelerating cineâ€MR imaging in mouse hearts using compressed sensing. Journal of Magnetic Resonance Imaging, 2011, 34, 1072-1079.	3.4	39